fMRI correlates of subjective reversals in ambiguous structure-from-motion

Elliot D. Freeman

City University, London, United Kingdom

Philipp Sterzer

Department of Psychiatry, Charité University Hospital, Berlin, Germany

Jon Driver

Wellcome Trust Centre for Neuroimaging & Institute of Cognitive Neuroscience, University College London, United Kingdom

We used fMRI to examine the neural correlates of subjective reversals for bistable structure-from-motion. We compared transparent random-dot kinematograms depicting either a cylinder rotating in depth or two flat surfaces translating in opposite directions at apparently different depths. For both such stimuli, the motion of dots on the different apparent depth planes typically appears to reverse direction periodically on prolonged viewing. Yet for cylindrical but not flat stimuli, such subjective reversals also coincide with apparent reversal of 3D rotation direction. We hypothesized that the lateral occipital complex (region LOC), sensitive to 3D form, might show greater event-related activity for subjective reversals of cylindrical than flat stimuli; conversely, motion-sensitive hMT+/V5 should respond in common to subjective reversals for either type of stimuli, as both are perceived as changes in planar motion. We obtained an event-related measure of neural activity associated with subjective reversals after first factoring out block-related differences between cylindrical versus flat stimuli (and thereby the associated low-level blocked stimulus differences). In support of our hypothesis, only the cylindrical stimuli produced reversal-related activity in contralateral human LOC. In contrast, the hMT+/V5 complex was activated alike by subjective reversals for both cylindrical and flat stimuli. Intriguingly, V1 also showed (contralateral) specificity for rotational reversals, suggesting a possible feedback influence from LOC. These results reveal specific neural correlates for subjective switches of 3D rotation versus translation, as distinct from subjective reversals in general.

Keywords: fMRI, human vision, multistability, structure-from-motion

Introduction

During prolonged viewing, the subjective appearance of ambiguous or "multistable" stimuli can switch spontaneously (e.g., Blake & Logothetis, 2002; Leopold & Logothetis, 1999; Sterzer, Kleinschmidt, & Rees, 2009). Pioneering electrophysiological animal studies (Bradley, Chang, & Andersen, 1998; Leopold & Logothetis, 1996) and human functional imaging (fMRI) studies (e.g., Castelo-Branco et al., 2002; Frith, Perry, & Lumer, 1999; Kleinschmidt, Buchel, Zeki, & Frackowiak, 1998; Lumer, Friston, & Rees, 1998) have successfully used multistable stimuli to identify neural responses associated with a purely subjective change in the appearance of a stimulus, as distinct from objective changes in the physical stimulus. Many human fMRI studies have focused either on binocular rivalry between different patterns presented dichoptically (e.g., Lumer et al., 1998; Polonsky, Blake, Braun, &

Heeger, 2000; Tong, Nakayama, Vaughan, & Kanwisher, 1998) or two-dimensional ambiguous motion stimuli that may appear to switch apparent direction of motion spontaneously on the frontoparallel plane (Muckli et al., 2002; Sterzer & Kleinschmidt, 2005, 2007; Sterzer, Eger, & Kleinschmidt, 2003; Sterzer, Russ, Preibisch, & Kleinschmidt, 2002). Recent fMRI research has also considered the third dimension, using random-dot kinematograms (RDK) to create ambiguous rotational motion in depth (Brouwer & van Ee, 2007). However, while most studies have examined just a single type of bistable stimulus, the present study compared two different bistable stimuli, which each evoke qualitatively distinct switch percepts. We compared translational 2D versus rotational 3D motion in flat versus cylindrical RDKs (see Figure 1 and online movie demonstrations). We thus aimed to contrast the distinct neural correlates of subjective switches of rotation versus translation.
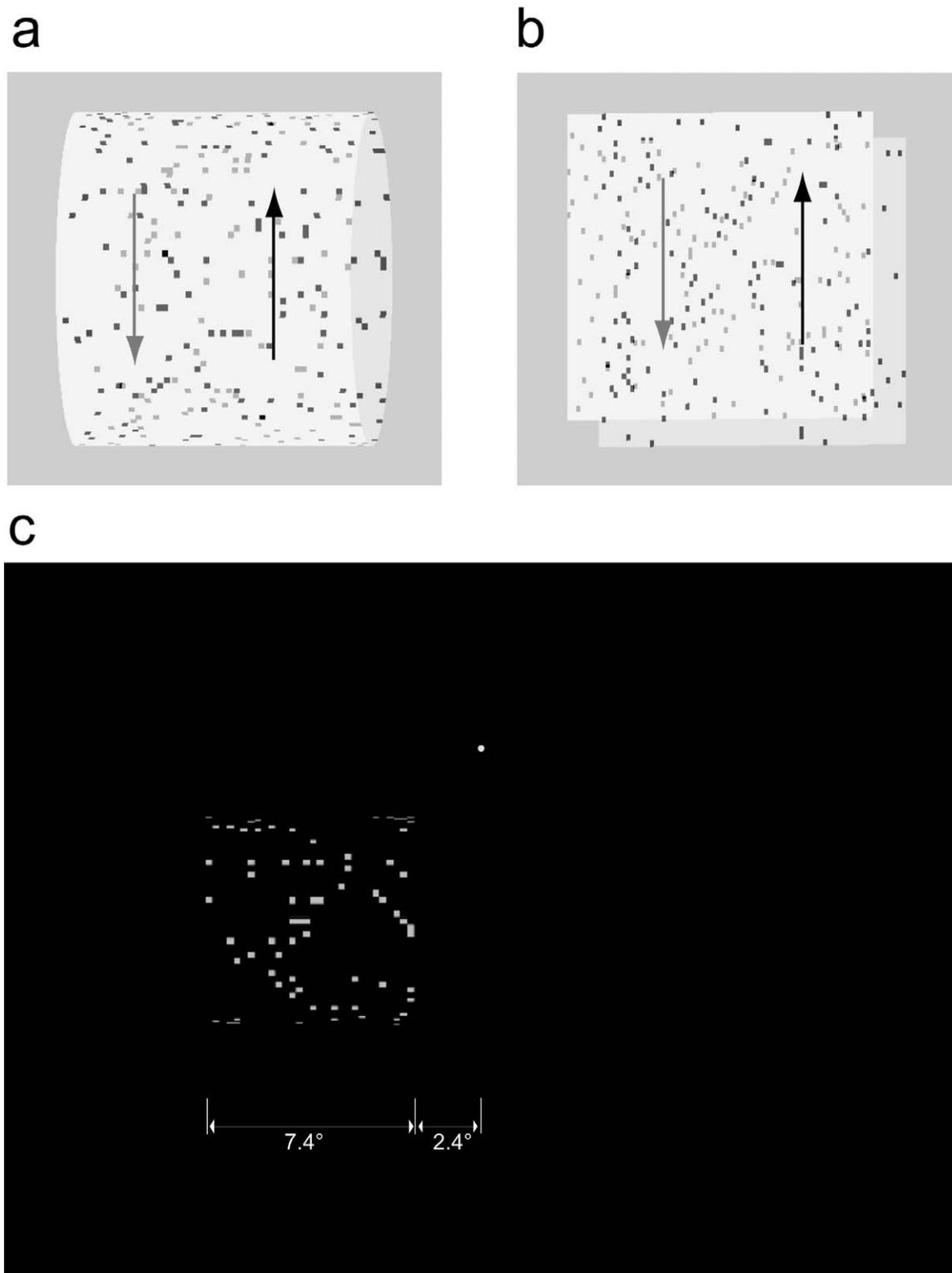
Figure 1. Examples of stimuli used. (a and b) Schematics of cylindrical and flat RDK stimuli with pictorial 3D cues (not present in experiment) added for illustration. Arrows indicate directions of dot motion for "front" and "back" surfaces; arrow curvature schematically illustrates motion in 3D rather than purely 2D motion. (c) Snapshot of a typical display with dimensions indicated in degrees of visual angle.

In a typical RDK, two superimposed fields of dots are presented moving coherently in opposite directions, typically creating the appearance of two transparent surfaces separated in depth, (i.e., the kinetic depth effect, Wallach & O'Connell, 1953). These surfaces can either be made to appear flat (Nawrot & Blake, 1989; Qian, Andersen, & Adelson, 1994) or contoured in depth (e.g., see Figure 1). The latter contoured effect is created by spatially modulating the dot aspect ratio and/or drift speed of the dots (Andersen & Bradley, 1998; Nawrot & Blake, 1989; Treue, Husain, & Andersen, 1991). This can create the impression of a transparent rotating 3D cylinder (as studied here) or other 3D shapes such as a rotating sphere (not studied here, but see Brouwer & van Ee, 2007).

Cylindrical and flat stimuli both induce spontaneous reversal of the assignment of dot-motion directions (e.g., upward versus downward) to specific depth planes (closer versus further) which remains ambiguous in the absence of strong depth cues such as binocular disparity or pictorial occlusion (Nawrot & Blake, 1989). For example, if at one moment upward-moving dots appear to be closer to the observer than downward-moving dots, at the next moment the apparently closer dots now appear to be moving downward and the more distant dots upward. While both cylindrical and flat stimuli share such switching behavior in common, a spontaneous reversal for the cylindrical stimulus uniquely entails a reversal in apparent 3D rotation. The impression when viewing the cylindrical stimulus is akin to a transparent "wheel" rolling either toward or away from the observer (i.e., with the front surface moving downward or upward, respectively). There is no such apparent rotational reversal when a subjective switch arises for the flat stimulus. It is the neural correlate of this subjective difference that the present study sought to isolate primarily, although further contrasts and conclusions were also possible (see following).

Flat and cylindrical stimuli obviously differ in low-level stimulus properties, but as explained after the next section, our fMRI design could subtract out all such low-level physical differences between the two classes of stimuli, which allowed us to isolate and compare the event-related brain response to purely subjective motion reversals for cylindrical versus flat stimuli. First, we briefly survey the role of two important dorsal and ventral brain areas, namely, the human MT complex (hMT+/V5) and Lateral Occipital Complex (LOC). These regions, which could be conveniently functionally localized for the purpose of a region-of-interest (ROI) analysis, have both been implicated in 3D structure from motion, though their precise roles remain uncertain. Later, we will consider other important parietal (Beer, Watanabe, Ni, Sasaki, & Andersen, 2009; Brouwer & van Ee, 2007; Kriegeskorte et al., 2003; Murray, Olshausen, & Woods, 2003;

Orban, Sunaert, Todd, Van, & Marchal, 1999; Vanduffel et al., 2002) and temporal regions (Beauchamp, Lee, Haxby, & Martin, 2002, 2003) in the discussion of our whole-brain analyses.

Brain regions potentially implicated in structure-from-motion

The defining property of structure-from-motion is that perception of form emerges from properties of visual motion, implying some synergy between mechanisms sensitive to motion and form (Kourtzi, Krekelberg, & van Wezel, 2008). Previous physiological and fMRI studies have revealed distinct brain regions involved in motion versus form processing, which have traditionally, but not exclusively, been associated with dorsal or ventral visual pathways, respectively (Braddick et al., 2001; Kourtzi et al., 2008; Mishkin, Ungerleider, & Macko, 1983).

In the dorsal pathway, the hMT+/V5 complex shows special sensitivity to coherently versus incoherently moving dots (e.g., Braddick, O'Brien, Wattam-Bell, Atkinson, & Turner, 2000; Braddick et al., 2001; Parker & Newsome, 1998; Rees, Friston, & Koch, 2000; Smith, Wall, Williams, & Singh, 2006). In monkeys, the analogous area is also activated by RDK displays that produce the perception of two transparent flat sheets translating in opposite directions at different disparity-defined depth planes (Bradley, Qian, & Andersen, 1995). Moreover, hMT+/V5 also responds well to "stereo-motion" induced by changes in surface depth (Likova & Tyler, 2007), as well as depth and structure defined by motion (Andersen & Bradley, 1998).

Such past results make hMT+/V5 an a priori region-of-interest (ROI) here for our novel comparison of subjective reversals in cylindrical versus flat stimuli. Both these types of stimuli involve perceiving coherent dot motion for perceptually distinct near versus far depth planes, which can subjectively reverse. Given this commonality, hMT+/V5 may respond similarly for subjective reversals in both cylindrical and flat stimuli. It remains unknown to what extent the hMT+/V5 complex may additionally represent properties of surface curvature and rotation in depth (which apply only for the cylindrical but not the flat stimuli here). Bradley et al. (1998) reported that cells in monkey MT correlated with perceived surface order for rotating SFM cylinders (and subjective reversals thereof). Furthermore, Andersen and Bradley (1998, their p. 227) also mentioned unpublished physiological data apparently showing that monkey MT activity correlates with perceived surface order in flat, transparent, dot-motion stimuli. However, it appears there was no attempt to directly compare subjective reversals in

cylindrical stimuli versus flat stimuli, as undertaken here for the first time with human fMRI.

Regarding rotational motion, region MST within the hMT/V5+ complex is activated preferentially by 2D rotation on the frontoparallel plane, as well as other patterns of optic flow (e.g., Morrone et al., 2000; Smith et al., 2006). In some studies, stronger activation was found within hMT+/V5 for rotating structure-from-motion stimuli, compared to static or 2D translating stimuli (Orban et al., 1999; Vanduffel et al., 2002). However, the nature of the contrasts often used in such studies can typically leave it uncertain which particular aspects of the structure-from-motion stimuli (e.g., rotation, motion in depth, 3D structure, or other low-level stimulus differences) were most critical in driving the activation.

MT+/V5 has been implicated in other studies of subjective reversals in perceived rotation direction during constant viewing of one type of ambiguous, rotating structure-from-motion stimuli (Bradley et al., 1998; Dodd, Krug, Cumming, & Parker, 2001; Grunewald, Bradley, & Andersen, 2002). For example, a recent fMRI study successfully used multivariate analysis to distinguish between alternative directions of SFM sphere-rotation based on patterns of activity within MT+, along with other dorsal visual and parietal areas (Brouwer & van Ee, 2007). In principle, however, similar results might potentially have been found with flat transparent motion stimuli which also exhibit spontaneous subjective switches of motion direction at different depth planes, but that was not tested.

Along the ventral visual pathway, Lateral Occipital Complex (LOC) can also show greater response to 3D structure-from-motion than to 2D motion (Murray et al., 2003; Orban et al., 1999; Paradis et al., 2000; Preston, Kourtzi, & Welchman, 2009; Vanduffel et al., 2002; Welchman, Deubelius, Conrad, Bulthoff, & Kourtzi, 2005). LOC activity has further been associated with dynamic stimuli for perception of globally coherent (versus incoherent) motion (Moutoussis, Keliris, Kourtzi, & Logothetis, 2005) and for apparent rotational motion between different successive views of a 3D object (Weigelt, Kourtzi, Kohler, Singer, & Muckli, 2007) compared to static superimposed views. LOC can also respond selectively to 3D or inferred-3D form with static images (e.g., Grill-Spector, Kourtzi, & Kanwisher, 2001; Kourtzi, Erb, Grodd, & Bulthoff, 2003; Moore & Engel, 2001) in addition to showing its well-known preference for structurally coherent over incoherent static images of natural objects (Grill-Spector et al., 2001; Kanwisher, Chun, McDermott, & Ledden, 1996; Tootell et al., 1995). What remains unclear is to what extent LOC sensitivity to structure-from-motion reflects a preference for 3D motion or just the coherent 3D structure implicit in that motion (such as cylindrical form). This issue could be addressed here

by measuring neural correlates of subjective switches in 3D rotation (versus 2D translation) after discounting activity associated with static cylindrical (versus flat) structure implied by the motion (see following for further explanation).

For completeness, we also assessed any involvement of early retinotopic visual cortex (specifically, areas V1 and V2) in the subjective reversals. Two past studies of ambiguous perception using (strictly 2D) apparent motion stimuli reported some suppressive and excitatory, reversal-related correlates in early visual areas (Kleinschmidt et al., 1998; Sterzer & Kleinschmidt, 2005). However, those studies only used offline monitoring for eye movements (i.e., outside the scanner, rather than during scanning). Because eye movements can sometimes correlate with switches in bistable perception, if not monitored during scanning, this might introduce potential confounds for activity in earlier retinotopic cortex. Moreover, the Kleinschmidt et al. (1998) and Sterzer and Kleinschmidt (2005) studies had identified early visual areas only on the basis of anatomical landmarks. By contrast here, we used functional retinotopic mapping of meridians to identify the borders of V1 and V2 in each individual participant, in combination with online tracking of eye position (including measures of blinking and pupil diameter) throughout all scanning. We note that, while on the one hand, it might seem unlikely that early areas such as V1 and V2 (with small receptive fields) would be involved in the "global" aspects of structure-from-motion perception and in associated subjective reversals, on the other hand, the perception of each local dot does change after such a global subjective reversal. Therefore, feedback influences upon early visual cortex due to a subjective reversal remain possible, as assessed here for both the cylindrical and flat stimuli.

Separation of blocked stimulus and event-related subjective-reversal brain activations

We now explain how we attempted to obtain a pure measure of brain responses associated with subjective reversal events for cylindrical versus flat stimuli independently of the gross physical differences between them (such as their different dot velocities and dot aspect ratios; see Methods). Our experimental design aimed to achieve this by presenting cylinder and flat stimuli to observers in separate blocks while, in both cases, recording the times of subjective switch-events as indicated behaviorally by observers. We could then use the General Linear Model to first assess any *block-related* effects associated with the blocked physical differences between these two stimulus types and thereby regress out such stimulus-related variance from the dataset. We then went on to study *event-related*

Blood Oxygenation Level-Dependent (BOLD) activity related to subjective reversals for either type of block. By comparing this event-related BOLD response for the two different stimulus types (see also Sterzer et al., 2003), we could compare neural responses associated with subjective reversals for cylindrical versus flat stimuli. Note that with multistable stimuli such as those used here, subjective reversals are observed in the absence of any coinciding physical change in the stimulus, hence are generally attributed to perceptual rather than stimulus-driven factors (Blake & Logothetis, 2002; Leopold & Logothetis, 1999).

Methods

Participants

The eight participants (24–36 years, three female) were authors EF and PS plus six naïve observers who participated for monetary compensation with written informed consent in accord with local ethics and in adherence of the Declaration of Helsinki. All reported normal or corrected visual acuity. All passed screening for normal medical history and no MRI contraindications.

Stimuli

An LCD projector (NEC LT158, NEC Corporation, Beijing, China) back-projected stimuli onto a screen at the rear of the magnet bore. Video mode was 640×480 with screen refresh rate of 60Hz, and output was linearized using 8-bit software gamma-transformation. Observers lay supine in the scanner and viewed the screen via a mirror mounted on the head coil at a viewing distance of 62 cm. The screen subtended horizontal and vertical visual angles of 26° and 18°, respectively. Stimulus presentation and timing was controlled by a PC running MATLAB (Mathworks Inc., Natick, MA) and the COGENT 2000 toolbox (http://www.vislab.ucl.ac.uk/cogent.php; UCL Functional Imaging Laboratory, Institute of Cognitive Neuroscience, and Laboratory of Neurobiology, UK). Each display comprised one kinematogram positioned at a polar angle of 45° diagonally below and to either the left or right of a small blue fixation point at a Euclidian distance of 3.4° (of visual angle) to the nearest corner. Each kinematogram comprised two superimposed fields of randomly distributed square white "dots" (maximum 0.3° of visual angle along edges) moving coherently in opposite directions on a black background. Kinematogram dimensions were 7.4° square. The direction of dot motion was vertical, up, or down (Figures 1a and 1b). Animation frames were updated every 50 ms, and the whole sequence of 100 frames was looped repeatedly to produce continuous motion. Maximum motion speed of dots was 6° per second, and dot lifetime was seven display frames (350 ms). Dot density for each visible surface was 2.2% for all stimuli. Two different apparent surface-depth profiles were tested: cylindrical and flat (see Figures 1a and 1b, respectively). For cylindrical stimuli, monocular cues for surface-curvature in depth were introduced by modulating both the speed and aspect ratio of dots as they moved along their paths. To produce the appearance of a cylinder rotating around a horizontal axis, dots moving (vertically) toward the upper or lower edge (and thus in both the y-direction and also apparently in the z-direction orthogonal to the plane of the screen) simultaneously decelerated and compressed in the y-direction, reaching zero velocity and height at the edge of the cylinder (Figure 1a). For flat stimuli, all dots drifted at the same speed of 4° per second with a constant aspect ratio (Figure 1b).

Design and procedure

The task for participants was to indicate, by holding down one of two response buttons, whether the dots appearing to be on the surface closest to them in depth were moving up or down (similar to Freeman & Driver, 2006, but now inside the scanner). Responses were made with the index and middle fingers of the right hand using two keys on the MR-compatible button box. Subjects were instructed to hold down one key corresponding to their current percept (but to release both keys if uncertain, which happened very rarely, in only 1% of all frames). Subjects were thoroughly familiarized with the stimuli and task in at least one prior session outside the scanner, and all found the perceptual reports straightforward. There were four blocked stimulation conditions, representing the crossing of two independent variables: hemifield (left versus right of fixation) and stimulus type (cylindrical versus flat). The hemifield factor was included to allow determination of whether any key brain activations were hemifield-specific (e.g., contralateral to the visual stimulus) rather than more general.

In each of four scanning runs per subject, each of the four blocked conditions (cylindrical/flat $\times$ left/right) was presented once in its own 90-second block with each block followed by a 15-second rest interval during which only the fixation point was displayed. Order of blocks was counterbalanced between runs and between subjects but with the constraint that the stimulus should be presented within opposite hemifields for successive blocks.

fMRI acquisition

BOLD contrast image volumes were acquired on an Allegra 3T scanner (Siemens, Erlangen, Germany). There were four scanning runs for each subject, comprising 191 volumes, each sampled with a repetition time of 2.21 sec. Duration of one run was 7 minutes. Volumes had 34 slices of 2-mm thickness with a 1-mm gap between slices, giving a resolution of $3 \times 3 \times 3$ mm. A T1-weighted structural image was also acquired together with three additional standard functional localizer scans. To identify borders of early visual cortical areas (V1 and V2) via meridian mapping (which readily distinguished V1 and V2, but is less effective for distinguishing subsequent retinotopic areas), contrast-reversing checkerboard patterns were displayed with 45° segments covering either the horizontal or vertical meridian and extending bilaterally from fixation out to the edge of the screen (similar to Sterzer, Haynes, & Rees, 2006). To localize the hMT+/V5 complex, participants viewed an annulus of 24° diameter, centered on fixation, composed of either stationary dots or expanding and contracting random dots moving at 4° of visual angle per second (Smith et al., 2006; Sterzer et al., 2006). For both of the previous localizer sequences, stimuli were displayed for 17.68 s, alternating 10 times with either a blank screen for the meridian localizer or a static dot field for the motion localizer, displayed for 11.05 s ($TR = 2.21$, 34 slices per volume). For LOC, a standard localizer was used comprising images of whole static object pictures versus static scrambled object pictures (Kourtzi & Kanwisher, 2000) displayed in alternating blocks of 12 scans (1 Hz presentation frequency, monochrome images centered on fixation with visual angle $8° \times 8°$) interspersed by six rest scans, repeating nine times ($TR = 2.08$, 32 slices per volume). Note that all these localizers were completely independent of the main experiment; hence they define regions of interest (ROIs) in an unbiased manner.

fMRI data analysis

Data were analyzed with SPM2 (http://www.fil.ion.ucl.ac.uk/spm; UCL Functional Imaging Laboratory, UK). The first five images of each scanning run were discarded to allow for magnetic saturation effects. The remaining images were realigned and coregistered to individual participants' structural scans for analysis of early retinotopic areas (V1 and V2). In addition, for analysis of hMT+/V5 and LOC ROIs, images were spatially normalized into standard space (MNI) and spatially smoothed with a Gaussian kernel of 8-mm FWHM in accord with the standard SPM approach. (This normalization to MNI space allows comparison of coordinates here to those in past studies.) A high-pass filter was applied at 0.0048 Hz to remove low-frequency signal drifts.

Following this preprocessing, data were then entered into a general linear model (Friston et al., 1994) that included eight experimental regressors. Of these, there were four block-related regressors (for left cylinder, right cylinder, left flat, and right flat) modeling the 90-second blocked epochs between onset and offset of specific stimuli in specific hemifields. The four remaining regressors were event-related and modeled (again for each of the above four stimulation conditions respectively) the timing of response key presses (signaling subjective perceptual reversals; see also Freeman & Driver, 2006) as discrete zero-duration events. No distinction was made between "up" and "down" keys, and the onsets of these key presses were offset backward in time by 500 ms for all subjects to compensate for the likely response time in reporting switches (Freeman & Driver, 2006).

This design enabled us to compare event-related, subjective-switch activations for the four blocked stimulation conditions, after having already accounted for any block-related effects due to differences in physical stimulation between the conditions. Note that any variance attributed to one regressor is discounted for others within the general-linear-model of the SPM approach. Hence, the blocked regressors will take out any activation differences caused, for instance, by blocked physical stimulus differences between our cylindrical and flat stimuli, leaving the event-related activations to reflect activity associated with just the subjective switches in phenomenal percept.

Parameter estimates for each of the regressors were collated for voxels lying within prespecified regions of interest (ROIs) of direct relevance to our hypotheses. These regions of interest were defined in two steps. In the first step, the relevant cortical areas (i.e., V1 and V2, plus hMT+/V5 and LOC) were each identified on the basis of the standard independent localizer scans (see previous). The use of independent localizers allowed us to circumvent issues of circularity that can otherwise arise for some fMRI analyses (Kriegeskorte, Simmons, Bellgowan, & Baker, 2009). Mask volumes for each region of interest in early retinotopic visual cortex (left and right dorsal V1 or V2, representing the lower visual field as stimulated by the kinematograms here) were obtained by delineating the borders between visual areas using activation patterns from the meridian localizers. We subsequently went on to consider only those voxels within V1 or V2 that responded to our RDK stimulation (see following) hence selecting the retinotopically appropriate sectors of V1 and V2, after first distinguishing their borders via the meridian localizers. We followed standard definitions of V1 and V2 together with segmentation and cortical flattening of grey matter using MrGray software
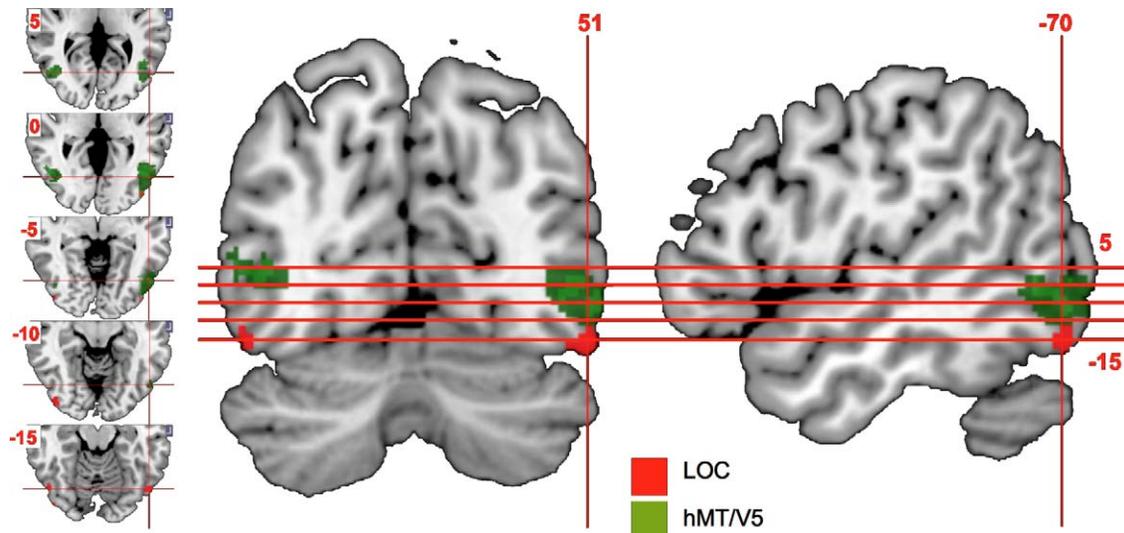
Figure 2. ROIs averaged across all observers, superimposed on a canonical brain, for LOC (in red) and hMT+/V5 (in green).

(Wandell Lab, Stanford, CA) (Teo, Sapiro, & Wandell, 1997; Wandell, Chial, & Backus, 2000). To identify regions hMT+/V5 or LOC, we obtained maps of the t-statistic for the independent localizer contrasts of moving-minus-static dots, or of whole-minus-scrambled objects respectively. These maps were thresholded at $p < 0.001$ uncorrected to provide mask volumes. Bilateral activations were observed for all subjects except three, for whom only unilateral activations in hMT+/V5 were identified at this threshold with the localizer. Clusters of contiguous above-threshold voxels were then selected from these maps with the additional criterion for LOC and hMT+/V5 that the coordinates of the centroids of each cluster had to be within ± 2 standard deviations (in Cartesian distance) from the previously published coordinates for hMT+/V5 (Hasnain, Fox, & Woldorff, 1998; Tootell et al., 1995; Watson et al., 1993) or LOC (Grill-Spector et al., 2001; Malach et al., 1995). For LOC, all resulting clusters were found to lie within the 2SD criterion range from the location of Ventral Posterior and Dorsal Posterior vertices described by Grill-Spector et al. (1998) but were outside the criterion range from the Ventral Anterior vertex.

The standard stimuli used in the localizer scans covered more of the visual field than the unilateral cylinder and flat stimuli used in the experimental scans. Many of the voxels in the initial ROIs, as defined by the initial localizers, might therefore represent unstimulated regions of the visual field, potentially decreasing signal-to-noise for our measures. As a second step, we therefore used functional data from the main experimental scans to limit our analyses to only those voxels within the anatomical areas already identified by the standard localizers that were specifically responsive to our RDK stimuli. These functional-volume masks were based on

the pooled response to *all* of the conditions relevant to block-related (or event-related) analyses versus baseline (see following). Such inclusive masking is a common procedure (Friston, Rotshtein, Geng, Sterzer, & Henson, 2006), which by virtue of pooling across all experimental conditions under study (i.e., here regardless of hemifield of presentation or cylinder versus flat stimulus) cannot impose any bias on the likelihood of subsequently finding any specific pattern of *differences* between conditions in our fully-balanced factorial design.

These inclusive masks were defined based on all the block-related or event-related activations against baseline. For the block-related analysis, t-maps were obtained for the main effect of stimulus epochs relative to rest epochs, thresholded at $p < 0.05$ uncorrected (for inclusiveness, i.e., so as to include liberally any voxels activated by our RDK stimuli). These maps were then masked inclusively with each of the independently defined volumes for V1, V2, hMT+/V5, and LOC as obtained from the first localizer step previously described.

For analysis of event-related differences between experimental conditions in hMT+/V5 and LOC, t-maps based on the standard localizers were masked inclusively with t-maps for the overall contrast of events relative to ongoing baseline (again thresholded at $p < 0.05$ uncorrected). We report following data only for subjects in whom ROIs could be reliably identified after this two-step process; only two subjects were excluded by these criteria. For those two subjects, LOC was hard to define using the two-step procedure, but similar results were obtained if instead all subjects ($n = 8$) were included, with the second step omitted for just those two subjects (i.e., unmasked functional localizer only). ROI locations for all subjects are illustrated in Figure 2 in a superimposed manner, for LOC (in red) and

	Mean (mm)			SD (mm)			
	x	*y*	*z*	*x*	*y*	*z*	*N*
Left hemisphere							
MT	−45	−69	3	2	6	1	5
LOC	−45	−77	−5	5	8	4	5
Right hemisphere							
MT	47	−72	1	3	7	3	6
LOC	46	−78	−2	4	9	6	3

Table 1. Talairach coordinates of MT and LOC regions of interest, averaged across subjects with standard deviations. *Notes*: The right-most column shows the number of subjects whose activations met the two-step criteria for identification of each ROI (see text for details and Figure 2).

hMT+/V5 (in green), in stereotactic (MNI) space, as also summarized in Table 1.

For event-related analysis of early retinotopic areas V1 and V2, event-related *F*-maps rather than *t*-maps were used to mask the initial individual ROIs identified using the standard meridians localizer as previously described. This was done given past reports that subjective switches (unlike blocked stimulation) can sometimes be associated with some transient *de*activations of early visual cortex, not just activations (Kleinschmidt et al., 1998; Sterzer & Kleinschmidt, 2005).

For each subject, mean estimates of percentage BOLD signal change were extracted for each of the block-related and event-related regressors, averaging across voxels and scanning runs within each relevant block-related or event-related ROI. For event-related analyses, we initially modeled events using the canonical hemodynamic response function (HRF) provided by SPM2, comprising a linear combination of two gamma functions, one modeling the peak and the other modeling the undershoot of the typical BOLD impulse response. This function reached a peak at 4.42 sec and a minimum at 15.5 sec. For completeness, we also modeled the time course of event-related activity using a Finite Impulse Response function (Dale, 1999; Ollinger, Shulman, & Corbetta, 2001). These procedures were all implemented by the MARSBaR toolbox (Brett, Anton, Valbregue & Poline, 2002), following the preprocessing previously described. The FIR analysis used five separate box-car regressors, each of 2.21 sec (equal to the TR), and each staggered in time by 2.21 sec. This was considered sufficient to capture the initial BOLD impulse elicited by a switch event, judging by the shape of a typical HRF. The estimated coefficients of each of these regressors can then be used to reconstruct the event time course. This FIR approach imposes no assumptions about the specific form of the hemodynamic response function, so can be more efficient at capturing the BOLD response to neural events whose precise onsets may be difficult to specify exactly, as for subjective switches in phenomenal perception. This approach to the fMRI data thus complements the standard SPM approach while making fewer assumptions.

Eye tracking

Eye data were acquired during scanning using remote-optics infrared eye tracking (ASL 504, Applied Science Laboratories, Bedford, MA). We excluded from the eye analysis any blinks or signal dropouts (i.e., pupil diameter = 0) and also apparent deviations of eye position greater than 10° of visual angle from the fixation point indicative of suboptimal calibration. Note that this latter exclusion zone preserved eye recordings anywhere within the critical stimulus display area. Eye recordings were excellent in six of the subjects, but for two subjects much of the eye data were rejected by these criteria due to poor signal/noise ratio with their particular eyes using this tracker. Offline analysis was conducted using the ILAB toolbox for Matlab (Gitelman, 2002).

Results

Behavioral

A common signature of bistable perception is that durations between successive subjective switches tend to fall within a gamma distribution (Borsellino, De Marco, Allazetta, Rinesi, & Bartolini, 1972). To assess whether our data also followed this pattern, we pooled data across subjects after normalizing (by taking the interswitch epoch duration data for each subject in each condition then dividing each of these datasets by its own mean to obtain distributions that were all centered on 1). We then tested goodness of fit to a gamma function (see histograms and fits in Figure 3a). A Kolmogorov-Smirnov test revealed no significant deviations from the gamma distribution for any of the four conditions (all $p > 0.1$). In contrast, all conditions
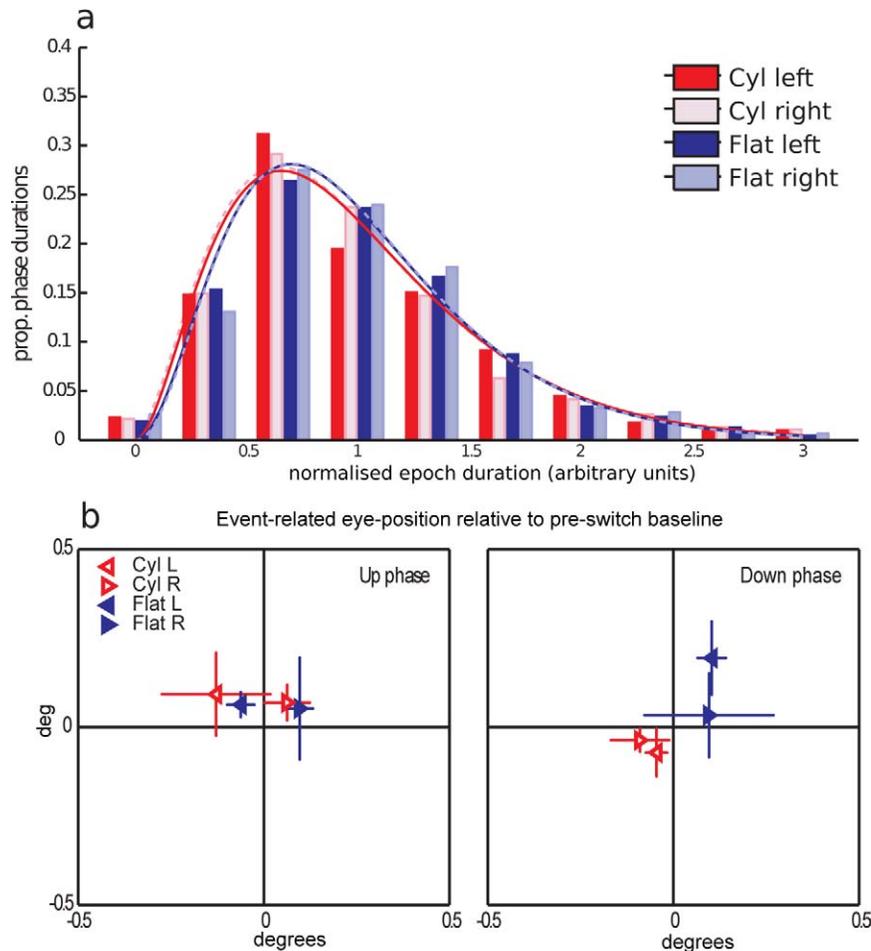
Figure 3. Behavioral data. (a) Histograms of normalized durations of phase intervals (in arbitrary units) between subjective switches for each of the four experimental conditions, with best-fitting gamma functions. (b) Mean eye positions per condition during 1 sec period immediately following a switch, relative to the period 500 ms before the switch, with standard error.

showed significant deviations from a Gaussian distribution (all $p < 0.005$). Mean R^2 values and standard deviations for the goodness of fit of gamma versus Gaussian distributions were as follows: mean gamma $R^2 = 0.45 \pm 0.06$ sd; mean Gaussian $R^2 = 0.32 \pm 0.07$ sd. Across subjects, goodness of fit was significantly higher for the gamma distribution ($t[7] = 2.67$, $p < 0.03$). We next tested for any consistent differences in the shape of the distribution between conditions or between "upward" versus "downward" phase durations. Parameter estimates (λ and r) for the fitted gamma functions were obtained for each subject in each condition and entered into two separate ANOVAs, with hemifield (left versus right), stimulus type (cylindrical versus flat), and indicated direction of rotation ("upward" versus "downward") as repeated-measures factors. There were no significant main effects or interactions. Similar analyses were performed for the means and geometric means of phase durations (means: $M = 5652$ ms, $SD = 1138$ ms; geometric means: $M = 2057$ ms, $SD = 501$ ms), again with nonsignificant

results (all $p > 0.1$). Thus, as with previous studies of bistable perception, subjective switches were well-described by a gamma function whose properties were similar for the two hemifields and the two stimulus types tested here.

Eye tracking

For analysis of block-related effects, mean X and Y eye coordinates were calculated across blocks for each of the four conditions. X and Y eye positions were then entered into separate repeated-measures ANOVAs, each with two factors: stimulus type (cylindrical versus flat) and hemifield of presentation (left versus right). There were no significant main effects or interactions. The mean eye positions (and standard errors) for X dimension, in degrees of visual angle, were as follows (negative values denote leftward deviations): Cylinder Left, −0.52 (0.13); Cylinder Right, 0.06 (0.27); Flat Left, 0.20 (0.18); Flat Right, 0.66 (0.3). For the Y
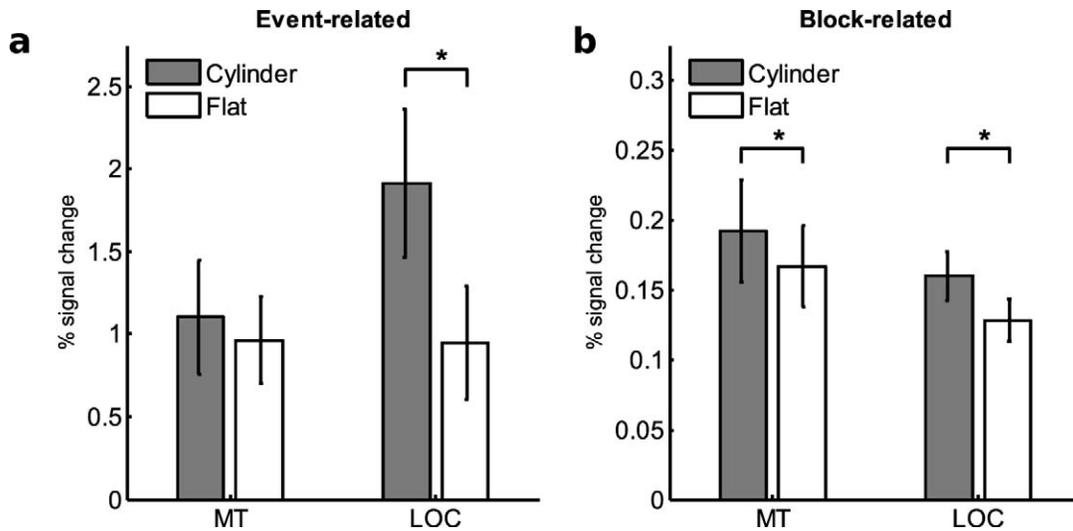
Figure 4. Estimated percentage BOLD signal change within LOC and hMT+/V5 ROIs for contralateral stimulation, averaged across participants. (a) Event-related results for purely subjective reversals, showing a significant interaction between stimulus type and ROI. (b) Block-related results for different stimulus types. Asterisks indicate statistical significance of planned comparisons at $p < 0.05$. Error bars represent one unit of standard error. Dark and light bars are for cylinder and flat conditions, respectively.

dimension: Cylinder Left, 0.54 (0.87); Cylinder Right, −0.07 (0.33); Flat Left, −0.62 (0.86); Flat Right, 0.15 (0.44). As well as this block-related analysis, we also conducted an event-related analysis, averaging eye positions and also pupil diameter and blink frequency across epochs beginning 500 ms before a key press and terminating 1000 ms thereafter. The pre-event data were averaged over the 500 ms prior to the sampling window to provide a baseline to which the postevent data were then referenced. Separate analyses were conducted for "up" versus "down" keys for each of the four conditions (see Figure 3b). For statistical analysis of these event-related eye data, there were four factors: cylindrical/flat, left/right, up/down response key, and time (50-ms time bins). There were no significant main effects or interactions for either the X or Y eye coordinates, nor for pupil diameter or blink frequency. We also analyzed saccade velocities. As their distributions were markedly skewed toward higher velocities, we computed geometric mean velocities for each subject and condition. There were no significant differences in average saccade velocities between stimulus types or locations. There was therefore no evidence to suggest that subjective perceptual switches (or stimulus types) were accompanied by consistent changes in any of the eye parameters here.

Finally, we tested whether there were systematic differences in eye velocity between conditions, which might have been caused by smooth pursuit or optokinetic movements induced by the moving stimuli. Gaze data were first split into epochs of 3500 ms beginning 500 ms before each key press and binned separately for "up" and "down" responses, and for

each stimulus type. Eye velocity was computed by first filtering out blinks and saccades (identified as eye movements whose initial eye velocities exceeded 30°/sec for a minimum duration of 35 ms, following Biscaldi & Otto, 1993), and then differentiating eye positions over 20-ms intervals. Mean horizontal and vertical velocities were then summarized for each stimulus and response type. Two-way repeated-measures ANOVAs revealed no significant differences for either measure. These results may help to allay any concerns that BOLD effects from fMRI might be causally related to transient changes in nonspecific arousal (as indexed by pupil diameter), to saccades, pursuit, or to blinking behavior around the time of a reported subjective switch.

fMRI data: ROI analyses of subjective switches for the different stimulus types in contralateral areas

An initial repeated-measures ANOVA compared event-related BOLD responses for subjective switches with cylinder versus flat stimuli between our four contralateral regions of interest (V1, V2, MT+/V5, and LOC). There was a significant interaction between region and stimulus type ($F[3, 15] = 7.01$, $p < 0.005$), indicating that subjective switches for the cylinder versus flat condition impacted differentially on these brain areas. To further address our hypothesis regarding the possible specificity of LOC (versus MT+/V5) for subjective reversals in 3D rotation (which arose only for the cylindrical, but less for the flat stimuli), we also

compared cylindrical versus flat reversals for just the contralateral hMT+/V5 and LOC regions of interest. The interaction term was again significant ($F[1, 5] = 10.52$, $p < 0.05$). As shown in Figure 4a, this arose because LOC showed a BOLD increase specific to cylindrical, but not flat subjective reversals; by contrast, hMT+/V5 showed a BOLD increase for either type of reversal. Planned pairwise comparisons of event-related activations in relation to subjective switches for each stimulus type showed a significant difference between cylinder and flat stimuli in contralateral LOC ($t[5] = 2.57$, $p < 0.05$), but not in contralateral hMT+/V5 ($t[5] = 0.28$, $p < 0.8$, n.s.), thereby leading to the significant interaction observed.

An analogous ANOVA just for early visual areas (contralateral V1 versus V2) also showed a significant interaction between stimulus type and ROI ($F[1, 5] = 14.04$, $p < 0.01$) with higher activation for cylinder in V1 (cylinder versus flat means $\pm$ standard error: 1.33 ± 0.77, 0.92 ± 1.01) compared to V2 that tended in the opposite direction (0.74 ± 0.41, 1.55 ± 0.62).

A recent study suggests that individual differences in frequency of SFM rotation-reversals can correlate with brain morphology (Kanai, Bahrami, & Rees, 2010). In light of this, we assessed whether individual differences in our BOLD measure of switch-evoked transients (percentage signal change) correlated with individual differences in our behavioral measure of epoch duration. We tested the correlation for each ROI and stimulus type, using mean and geometric mean epoch durations (not normalized) calculated for each subject. There were no significant correlations (all $p > 0.1$).

fMRI data: reversal-related activations for each ROI, by hemifield and against time

Having found significant differences in the response to cylinder versus flat stimuli between areas, we next assessed within each area whether brain responses associated with subjective-reversal events in our ROIs were specific to the hemifield of the perceived stimulus (i.e., arising contralaterally) or arose more generally regardless of that (which might then be potentially consistent with less-specific factors such as arousal). We also looked at the time course of the reversal-related BOLD signals for each ROI via the FIR approach. The latter approach makes no assumptions about the nature of the BOLD HRF, unlike the standard SPM approach, giving a "rawer" view of the BOLD time course.

For the FIR analysis, a three-way ANOVA on each ROI (i.e., LOC, MT+/V5, V2, or V1) had factors of laterality (ipsilateral or contralateral to the currently viewed RDK); stimulus type (cylindrical or flat, but after the blocked impact of that stimulus factor had been regressed out to leave only the event-related brain response to subjective-reversal); and time (five successive bins of 2.21 seconds). For LOC, this revealed a three-way interaction between contralaterality, stimulus type, and time ($F(4, 20) = 3.0$, $p < 0.05$). As shown in Figure 5a, LOC activity associated with a subjective reversal in perceived contralateral cylinder rotation developed to a peak at around 6 seconds, then decayed over a period of about 12 seconds. The other three conditions (ipsilateral cylinder reversals or flat reversals in either hemifield) all showed less temporal modulation. No such interaction pattern was found for the FIR analysis of hMT+/V5 ($F[4, 20] = 0.5$, n.s.) despite significant main effects of time ($F[4, 20] = 16.6$, $p < 0.0001$) and laterality ($F[1, 5] = 37.3$, $p < 0.002$); see Figure 5b. Thus, hMT+/V5 showed an event-related response for both cylindrical and flat subjective reversals alike with some contralateral specificity. Note that hMT+/V5 showed some weak ipsilateral response in accord with past research (Smith et al., 2006), but nevertheless a significantly stronger contralateral response and no differentiation between cylindrical or flat subjective reversals. By contrast, LOC (unlike hMT+/V5) showed a stronger response for subjective reversals involving a change in 3D rotation in particular (i.e., for the cylindrical case only), also contralaterally. This pattern of results confirms our hypothesis (see Introduction) that LOC may be implicated in 3D transformational aspects of structure-from-motion perception, whereas hMT+/V5 may not distinguish the two types of subjective reversal here. Direct comparison of the contralateral response between hMT+/V5 and LOC showed a significant interaction of ROI with stimulus type ($F[1, 5] = 16.91$, $p < 0.01$) due a cylindrical/flat subjective-switch difference emerging only for LOC in accord with the previous SPM analysis using the canonical HRF.

Analogous analysis of FIR results for V1 or V2 revealed a significant two-way interaction in V1 between stimulus type and laterality ($F[1, 7] = 7.09$, $p < 0.03$); see Figure 5c. Similarly to LOC, subjective reversals of cylinder rotation specifically induced a greater transient response in V1 contralateral to the hemifield of stimulation, compared to flat stimuli in either hemifield or to ipsilateral cylinder reversals. No such interaction pattern was evident for V2 (Figure 5d).

The same patterns of results were found for V1/V2 in a conventional HRF-based event-related analysis with factors of laterality and region, but now without time as a factor, unlike the more detailed FIR analyses. This yielded a significant two-way interaction for laterality $\times$ stimulus type in V1 ($F[1, 7] = 7.354$, $p < 0.05$) and a trend toward a similar interaction pattern for LOC ($F[1, 5] = 5.9$, $p = 0.06$), but not for the other ROIs.
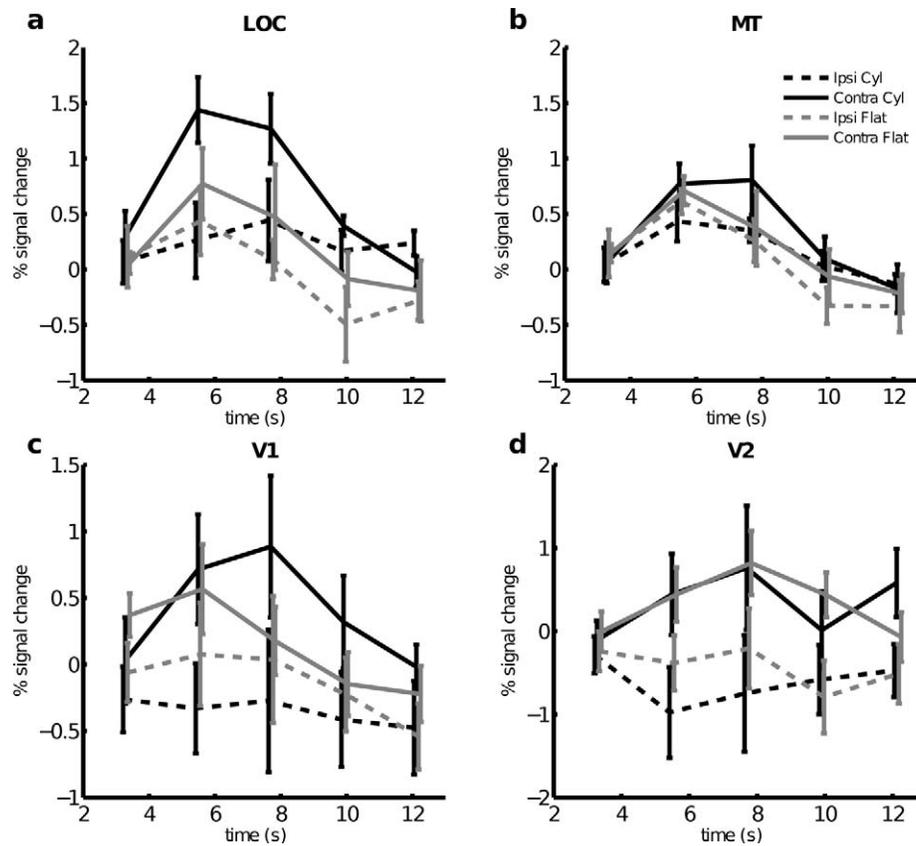
Figure 5. Results of event-related time course (FIR) analysis for selected ROIs, comparing activation both contralateral and ipsilateral to stimulation. (a) LOC. (b) hMT+/V5. (c) V1. (d) V2. Lines of different colors correspond to different conditions, as indicated by the key at upper-right of (b). Error bars represent one unit of standard error.

fMRI data: block-related BOLD in relation to the stimulus

Estimates of block-related percentage signal change in BOLD were compared for cylindrical versus flat stimuli in LOC versus hMT+/V5 ROIs (initially always contralateral to the hemifield of stimulation). There was a significant main effect of stimulus type with cylinders evoking greater activation in both ROIs ($F[1, 7] = 12.64$, $p < 0.01$); see Figure 4b. Pairwise comparisons showed significantly greater activation for cylindrical minus flat stimuli in *both* contralateral areas (LOC: $t[7] = 3.2$, $p < 0.02$; hMT+/V5: $t[7] = 2.6$, $p < 0.04$). This blocked, stimulus-induced pattern therefore differs from the event-related pattern specific to subjective reversals, in that both LOC and hMT+/V5 show a preference for blocked cylindrical stimuli, but only LOC differentiated subjective-reversal events for cylindrical versus flat (see previous).

ANOVAs were conducted on each ROI separately with factors of blocked stimulus type and contralaterality. These showed a significant main effect of greater activation for blocked cylindrical than flat stimuli in both LOC ($F[1, 7] = 11.8$, $p < 0.01$) and hMT+/V5 ($F[1,$

$7] = 9.1$, $p < 0.02$), plus stronger activation for contralateral than ipsilateral blocked stimuli in both these areas (LOC: $F[1, 7] = 97.4$, $p < 0.0001$; hMT+/V5: $F[1, 7] = 22.1$, $p < 0.002$) with no significant interaction. For V1 and V2, ANOVAs on either region showed the expected strong effect of contralaterality (V1: $F[1, 7] = 61.9$, $p < 0.0001$; V2: $F[1, 7] = 56.3$, $p < 0.0001$), but no impact of blocked stimulus type and no interaction.

The block-related modulations were small compared to event-related ones (e.g., see Figure 4). To assess whether block-related effects had been estimated effectively and independently, we compared how well our data were fit by a "full" model comprising both event-related and block-related regressors, relative to a "reduced" model in which the block-related regressors were not entered. In all subjects and ROIs, R^2 values for model fits were significantly higher in the full model

	V1 and V2	SD	MT and LOC	SD
With blocks	0.64	±0.03	0.29	±0.04
Without blocks	0.41	±0.03	0.21	±0.02

Table 2. Goodness of fit values (R^2) for a full regression model and a reduced model eliminating the blocks regressor.

Contrast	Area	x	y	z	n voxels	z-score
Event-related						
Increase	R posterior LOC	51	−68	−5	20	3.76
	L MT+	−36	−68	7	24	3.62
Decrease	Cuneus Brodmann 18	10	−70	21	57	4.00
	Posterior Cingulate	10	−48	6	32	4.28
Block-related						
Cylinder	L MTG	−60	−52	0	103	4.04
Flat	R MTG	68	−30	−10	265	4.60

Table 3. Talairach coordinates and volume of areas showing increased or decreased activity ($p < 0.01$ corrected) associated with switch-events (see also Figure 4) or greater block-related activity for cylinder than flat stimuli.

(V1 and V2: $F[1, 7] = 287.30$, $p < 0.0001$; MT and LOC: $F[1,7] = 28.062$, $p < 0.001$; see Table 2), indicating that the inclusion of block-related regressors did indeed result in a reliably better model of the BOLD data. Indeed the interaction effect of critical interest (larger contralateral event-related response in LOC for reversals in cylinders compared to flat) was not significant in the reduced model without block-related regressors ($F[1, 5] = 3.5$, n.s., as compared to $F = 10.52$ as previously reported), suggesting that the full model had adequately modeled and partialed out block-related activity from the event-related effects.

Whole-brain analyses

Although all of our hypotheses had concerned specific ROIs (see previous), for completeness we also conducted conventional random effects analyses for selected *t*-contrasts across subjects across all voxels of the brain. Comparing the block-related response to cylindrical > flat stimuli revealed significant bilateral clusters in anterior middle temporal gyrus (MTG), ($p < 0.001$ for clusters of the observed size or greater, after correction for multiple comparisons; see Table 3 for Talairach coordinates and Figure 6).

A further whole-brain, random effects analysis examined BOLD activity positively associated with all switch-related events across subjects. This revealed two regions, significant at the cluster level at $p < 0.01$ corrected (see Table 3 and Figure 6). One was found in the left hemisphere within the region identified by the motion-functional localizer as hMT+/V5 and the other in the right hemisphere within the region identified by the objects-functional localizer as LOC. These locations were respectively within 2SD of published coordinates for V5 (Hasnain et al., 1998; Tootell et al., 1995; Watson et al., 1993) and LOC (Grill-Spector et al., 2001; Grill-Spector et al., 1998; Malach et al., 1995). The inverse contrast revealed significant clusters of switch-related suppression of activity in the right hemisphere within cuneus, Brodmann area 18 (putative V2) and also in posterior cingulate ($p < 0.001$ corrected). Previous studies have attributed a monitoring or evaluative role to posterior cingulate (Small et al., 2003; Vogt, Finch, & Olson, 1992). In the present context, the deactivation here might conceivably reflect interruption of a "default mode" of function prior to the subjective reversal (Raichle et al., 2001). No suprathreshold clusters were found for the event-related cylinder/flat contrast after correction at the
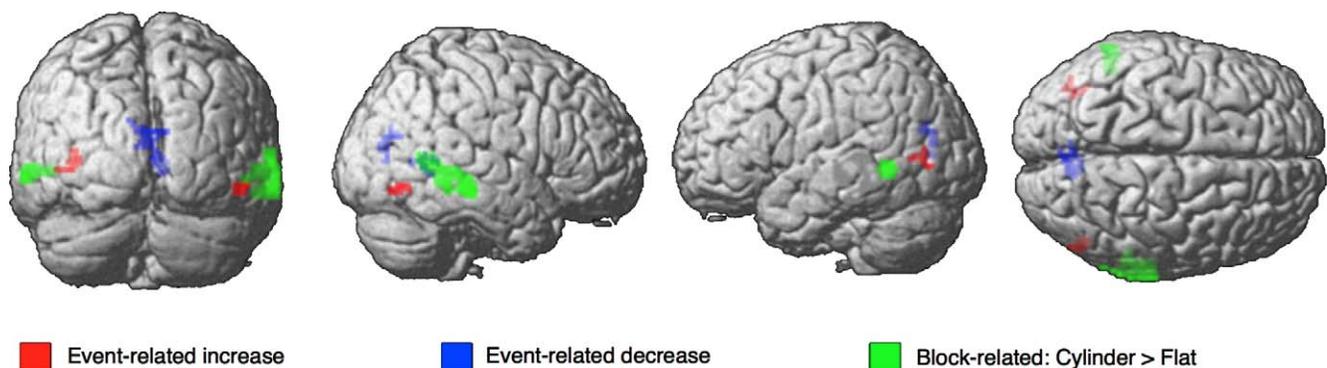

Figure 6. Results of whole-brain-corrected random-effects SPM analyses. Red and blue areas show increased and decreased activation during switch events respectively. Green areas show where block-related activity was greater for cylinder than flat stimuli. The locations of regions below the cortical surface may be inferred by comparing the different viewpoints.

whole-brain level, thus no areas beyond our independently identified ROIs were implicated.

General discussion

The present study makes several new contributions toward understanding the neural correlates of phenomenal perception for bistable random-dot structure-from-motion (SFM) displays. First, we were able to measure the distinct neural correlates of subjective switches in rotation versus just relative surface depth, in contrast to previous fMRI studies that typically focused only on 2D apparent motion (Sterzer & Kleinschmidt, 2005, 2007; Sterzer et al., 2003; Sterzer et al., 2002) or on subjective *states* in SFM rather than reversals per se (Brouwer & van Ee, 2007). Second, we could discount eye movements or other eye changes (i.e., blinks, pupil dilations) and also nonspecific arousal as a general explanation for the contralateral brain activations associated with subjective reversals in visual perception, yet still find robust switch-related transient activations across all of our regions of interest. Third, we contrasted subjective reversals for cylindrical versus flat SFM stimuli here, while separating any effects due to purely subjective reversals for these different types from blocked effects driven by physical stimulus differences, which were assessed here (and regressed out) by the blocked contrasts distinct from the critical event-related subjective-switch contrasts. This analysis highlighted a functional dissociation between two cortical regions: hMT+/V5 responded in a common manner to subjective reversals for both cylindrical and flat stimuli; in contrast, LOC showed increased activation specifically for subjective reversals of (contralateral) cylinders, which (unlike the flat stimuli) undergo reversals of 3D rotation direction. These results thus indicate that brain activation associated with subjective reversals can be specific to the change in perceived visual content, such as a 3D rotational reversal (as for LOC and V1). Our data thus reveal a new specificity in the cortical response to changes in subjective visual percepts.

Most past fMRI studies on 3D structure-from-motion contrasted stimuli that differed physically (Orban et al., 1999; Paradis et al., 2000; Vanduffel et al., 2002; Welchman et al., 2005). Such contrasts have revealed activations in areas such as hMT+/V5 and LOC, plus earlier retinotopic areas in some cases, which were correlated with differences in perceived 3D form (but were typically also confounded by stimulus differences). The present study similarly found higher block-related activity for cylindrical compared to flat stimuli in LOC and hMT+/V5 (see Figure 4b). This broadly agrees with past results, given that the

cylindrical stimuli may have led to greater perceived 3D depth and 3D motion than flat. However, simply comparing different stimuli in separate blocks inevitably raises the possibility that some of the resulting activation differences might reflect differences in stimulation rather than just in perception, such as the physically different patterns of dot motion and aspect ratio.

Other studies have looked within a single stimulus type for neural correlates of phenomenological reversals (Sterzer et al., 2003) or for distinct phenomenological states such as upward versus downward rotation or direction of apparent motion (Brouwer & van Ee, 2007). Such approaches (as for the subjective reversals studied here) can eliminate confounding physical stimulus differences. But if only one stimulus type (and thus one type of subjective reversal) is studied, it can be hard to determine if the results are specific to that type or not. A pioneering study by Brouwer and van Ee (2007) used multivariate image classification to identify brain regions sensitive to the difference between opposite, sustained subjective states of perceived rotation for a single type of SFM stimulus (spherical). Their results showed reliable discrimination in hMT+/V5 (among other regions, though they did not examine LOC). However, as with most fMRI studies, those authors used a single type of rotating SFM stimulus only. For their spherical stimuli, a reversal involves both reversal of dot-motion directions on different depth planes (as for both our flat and our cylindrical stimuli) *and* also a perceived change in 3D rotation (as for our cylindrical, but not flat stimuli), which leaves it uncertain which of these perceived properties were responsible for driving the state-related effects that they measured.

The present approach differed from those previously outlined by comparing reversal-related brain responses for two different stimulus types associated with qualitatively different perceptions. The event-related activity triggered by subjective reversals circumvents blocked stimulus confounds, as it reflects only subjective perceptual differences elicited spontaneously while the physical stimulus remained constant. The block-related regressors accounted for the differences between the physical stimulus types. Moreover, the direct comparison of cylindrical versus flat reversal-related activity will also be free from sensorimotor confounds associated with subjects' key presses indicating a perceptual switch (Sterzer et al., 2003), as such response-related activity should be equivalent for subjective reversals with the stimulus types contrasted here.

In some prior studies of bistable perception with neural measures, reversal-related activity cannot always be distinguished from possible effects of eye movements, blinks, or pupil dilations (see Kleinschmidt et

al., 1998; Sterzer & Kleinschmidt, 2005). But here, our concurrently recorded eye data revealed neither blocked nor switch-related differences between conditions, in terms of deviations from fixation during switches, pupil diameter, saccade velocity, smooth-pursuit behavior, or blinking. Moreover, the specific differential effects for cylinder versus flat stimuli found between ROIs, together with their specifically contra-lateral nature (see following), also weigh against any nonspecific explanations in terms of such oculomotor factors or indeed by any other nonspecific factors such as arousal. Instead, the pattern of switch-related activity seems to depend critically on the specific nature of the subjective switch, such as whether it involves a change in apparent 3D rotation or not.

A critical result in the event-related data arose for LOC, where activity was highest for subjective reversals with contralateral cylinders in particular. While there are some prior reports of contralaterality in the LOC when using peripheral stimuli (Niemeier, Goltz, Kuchinad, Tweed, & Vilis, 2005), to our knowledge the present study is the first to show that contralateral LOC can be selectively sensitive to purely subjective changes in apparent 3D dynamic rotations (as for the cylindrical RDKs here). The contralaterality of this selective response would not be expected if the event-related activity merely reflected some generalized peak of arousal caused by a perceptual switch or even some nonlateralized top-down perturbation signal that might theoretically cause a perceptual switch (Leopold & Logothetis, 1999). A lateralized event-related peak of activity might still in principle be caused by temporarily increased allocation of attentional resources to the location occupied by the suddenly reversing stimulus, as the subjective switch was relevant to the task the subject performed. But note that any such nonspecific attentional effect should be comparable for both cylindrical and flat stimuli, whereas we found differences in the associated event-related response in LOC (and also V1, see following).

The present region-specific, event-related effects of perceptual reversals appear to suggest functional differences between different cortical areas that may relate to the kind of perceptual transition that each can support. For example, on the one hand, the cylinder-specific lateralized activations in LOC for subjective switches may reflect the percept of (subjective) 3D rotation reversals, which arose for cylindrical, but not flat stimuli here. On the other hand, the more general event-related activations in hMT+/V5 (found in common for subjective reversals in both cylindrical and flat stimuli here) may presumably relate to the kind of subjective switch that both stimulus types have in common, namely subjective reversals of dot-motion direction on different depth planes.

A few prior studies have reported transient activity in early visual cortex in relation to subjective switches of motion perception (Kleinschmidt et al., 1998; Sterzer et al., 2006). However, those studies neither used retinotopic mapping to distinguish visual areas, nor applied eye tracking throughout scanning, unlike here. Kleinschmidt et al. (1998) contrasted epochs during which the percept was reported to be switching versus epochs where it appeared stable and found some reduced BOLD near the calcarine fissure. Sterzer and Kleinschmidt (2005) reported calcarine BOLD increases or decreases with the direction of this effect depending critically on whether the subjective switch was toward a percept consistent with or contrary to stimulus cues, respectively. In the present study, we observed reversal-related increases in activation in V1. Note that, unlike Sterzer and Kleinschmidt (2005), here both alternative percepts were always equally consistent with the stimuli.

Single-cell data from monkeys have suggested that V1 is not directly involved in generation of structure-from-motion (Grunewald et al., 2002), a conclusion apparently corroborated by human fMRI studies (Orban et al., 1999; Paradis et al., 2000; Vanduffel et al., 2002; Welchman et al., 2005). Yet here, V1 differentiated between subjective reversals for cylindrical versus flat RDK stimuli in an analogous manner as for LOC (compare Figure 5a and 5c). This impact on V1 might reflect feedback influences from LOC (or from further higher areas) when perceived 3D rotation reverses subjectively, possibly in accord with the consequent changes in interpretation for local dots. hMT+/V5 and V2 did not show this pattern. This selective activation of V1 concurs with prior evidence also suggesting a selective association between LOC and V1 for perception of coherent versus incoherent patterns of motion (Murray, Kersten, Olshausen, Schrater, & Woods, 2002). In that study, analogously to the present findings, only V1 was reliably associated with activity changes in LOC contingent on perceived coherent motion while areas identified as V2 or V3 showed no such significant change on average.

The highly selective patterns of activation associated with subjective reversals of cylinder motion here (which specifically activated contralateral LOC and V1 more than flat reversals) allows us to reject, empirically, any criticism that the event-related effects associated with subjective switches of cylinder versus flat percepts might somehow still just reflect differences between the stimuli themselves. The blocked effects of stimulus type were different in kind and did not selectively activate LOC or V1 for cylinders versus flat stimuli, unlike the subjective switches. Moreover, there was no actual stimulus change when subjective switches arose.

Parietal areas have been shown to be important in many past studies of structure-from-motion (SFM)

processing when comparing blocks of SFM stimulation against blocks of incoherent motion, or against 2D motion or static images (Beer et al., 2009; Brouwer & van Ee, 2007; Kriegeskorte et al., 2003; Murray et al., 2003; Orban et al., 1999; Vanduffel et al., 2002). In addition, there is recent fMRI evidence using an adaptation paradigm that regions in posterior parietal cortex can represent (and become selectively adapted to) distinct complex static 3D forms (Konen & Kastner, 2008). However, the present study found no evidence of significant parietal activation in our corrected whole-brain analyses. This seems likely to reflect the more subtle contrast examined here between two different types of SFM stimuli (cylindrical versus flat, instead of SFM versus none) in the context of a block-related design rather than an adaptation paradigm (Konen & Kastner, 2008), so our results need not be taken as evidence against involvement of parietal areas in other aspects of SFM perception.

One interesting area highlighted by our whole-brain analysis was middle temporal gyrus (MTG). This has previously been reported in the context of movies depicting tools undergoing their characteristic motion (versus not moving), whether conveyed by realistic movies or by point-light displays (Beauchamp et al., 2002, 2003). In light of the past data on MTG, it can be suggested that this region may respond more to our cylindrical than flat stimuli because the former yields a coherent single 3D object with a characteristic rotational motion that is uniquely constrained by its form while the flat stimuli are composed of two separate surfaces in which the motion of each is unrelated and arbitrary.

In conclusion, the present results identify specific fMRI responses within the human visual system for phenomenologically distinct types of subjective reversals in closely comparable, but subtly distinct types of structure-from-motion stimuli. Event-related comparison of reversal-related activity between two different types of RDK stimuli (rotating transparent cylinders versus translating flat surfaces) revealed lateralized specificity in LOC and also V1 for subjective reversals in 3D rotation, which was not apparent when comparing the different stimulus types in separate blocks. This extends knowledge about LOC, which has previously been associated with selectivity for structural properties of 3D stimuli, by now revealing an additional selectivity for dynamic or transformational 3D properties (Orban et al., 1999), such as rotation in depth. The results for LOC also contrasted with the more general reversal-related responses observed for both cylinder and flat stimuli alike within hMT+/V5 and V2. In addition to the specific response of LOC to subjective reversals in 3D rotational motion observed for just the cylindrical stimuli, our results provide new

evidence consistent with possible feedback of such reversal-related responses to area V1.

Commercial relationships: none.
Corresponding author: Elliot D. Freeman.
Email: elliot.freeman@city.ac.uk.
Address: City University, London, UK.

References

Andersen, R. A., & Bradley, D. C. (1998). Perception of three-dimensional structure from motion. *Trends in Cognitive Sciences, 2*, 222–228. [PubMed]

Beauchamp, M. S., Lee, K. E., Haxby, J. V., & Martin, A. (2002). Parallel visual motion processing streams for manipulable objects and human movements. *Neuron, 34*, 149–159. [PubMed]

Beauchamp, M. S., Lee, K. E., Haxby, J. V., & Martin, A. (2003). FMRI responses to video and point-light displays of moving humans and manipulable objects. *Journal of Cognitive Neuroscience, 15*, 991–1001. [PubMed]

Beer, A. L., Watanabe, T., Ni, R., Sasaki, Y., & Andersen, G. J. (2009). 3D surface perception from motion involves a temporal-parietal network. *European Journal of Neuroscience, 30*, 703–713. [PubMed]

Biscaldi, M., & Otto, P. (1993). Saccadic eye movements of dyslexic adults. *Neuropsychologia, 31*(9), 887–906. [PubMed]

Blake, R., & Logothetis, N. K. (2002). Visual competition. *Nature Reviews Neuroscience, 3*, 13–21. [PubMed]

Borsellino, A., De Marco, A., Allazetta, A., Rinesi, S., & Bartolini, B. (1972). Reversal time distribution in the perception of visual ambiguous stimuli. *Kybernetik, 10*, 139–144. [PubMed]

Braddick, O. J., O'Brien, J. M., Wattam-Bell, J.,

Atkinson, J., Hartley, T., & Turner, R. (2001). Brain areas sensitive to coherent visual motion. *Perception, 30*, 61–72. [PubMed]

Braddick, O. J., O'Brien, J. M. D., Wattam-Bell, J., Atkinson, J., & Turner, R. (2000). Form and motion coherence activate independent, but not dorsal/ventral segregated, networks in the human brain. *Current Biology, 10*, 731–734. [PubMed]

Bradley, D. C., Chang, G. C., & Andersen, R. A. (1998). Encoding of three-dimensional structure-from-motion by primate area MT neurons. *Nature, 392*, 714–717. [PubMed]

Bradley, D. C., Qian, N., & Andersen, R. A. (1995). Integration of motion and stereopsis in middle temporal cortical area of macaques. *Nature, 373*, 609–611. [PubMed]

Brett, M., Anton, J. L., Valbregue, R., & Poline, J. (2002). Region of interest analysis using an SPM toolbox (abstract). *Neuroimage, 16*, 372.

Brouwer, G. J., & van Ee, R. (2007). Visual cortex allows prediction of perceptual states during ambiguous structure-from-motion. *Journal of Neuroscience, 27*, 1015–1023. [PubMed] [Article]

Castelo-Branco, M., Formisano, E., Backes, W., Zanella, F., Neuenschwander, S., Singer, W., et al., (2002). Activity patterns in human motion-sensitive areas depend on the interpretation of global motion. *Proceedings of the National Academy of Sciences USA, 99,* 13 914–13 919. [PubMed] [Article]

Dale, A. M. (1999). Optimal experimental design for event-related fMRI. *Human Brain Mapping, 8*, 109–114. [PubMed]

Dodd, J. V., Krug, K., Cumming, B. G., & Parker, A. J. (2001). Perceptually bistable three-dimensional figures evoke high choice probabilities in cortical area MT. *Journal of Neuroscience, 21*, 4809–4821. [PubMed] [Article]

Freeman, E. D., & Driver, J. (2006). Subjective appearance of ambiguous structure-from-motion can be driven by objective switches of a separate less ambiguous context. *Vision Research, 46*, 4007–4023. [PubMed]

Friston, K. J., Holmes, A. P., Worsley, K. P., Poline, J. B., Frith, C. D., & Frackowiak, R. S. (1994). Statistical parametric maps in functional imaging: a general linear approach. *Human Brain Mapping, 2*, 189–210.

Friston, K. J., Rotshtein, P., Geng, J. J., Sterzer, P., & Henson, R. N. (2006). A critique of functional localisers. *Neuroimage, 30*, 1077–1087. [PubMed]

Frith, C., Perry, R., & Lumer, E. (1999). The neural correlates of conscious experience: an experimental framework. *Trends in Cognitive Sciences, 3*, 105–114. [PubMed]

Gitelman, D. R. (2002). ILAB: a program for postexperimental eye movement analysis. *Behavior Research Methods, Instruments & Computers, 34*(4), 605–612. [PubMed]

Grill-Spector, K., Kourtzi, Z., & Kanwisher, N. (2001). The lateral occipital complex and its role in object recognition. *Vision Research, 41*, 1409–1422. [PubMed]

Grill-Spector, K., Kushnir, T., Hendler, T., Edelman, S., Itzchak, Y., & Malach, R. (1998). A sequence of object-processing stages revealed by fMRI in the human occipital lobe. *Human Brain Mapping, 6*, 316–328. [PubMed]

Grunewald, A., Bradley, D. C., & Andersen, R. A. (2002). Neural correlates of structure-from-motion perception in macaque V1 and MT. *Journal of Neuroscience, 22*, 6195–6207. [PubMed] [Article]

Hasnain, M. K., Fox, P. T., & Woldorff, M. G. (1998). Intersubject variability of functional areas in the human visual cortex. *Human Brain Mapping, 6*, 301–315. [PubMed]

Kanai, R., Bahrami, B., & Rees, G. (2010). Human parietal cortex structure predicts individual differences in perceptual rivalry. *Current Biology, 20*, 1626–1630. [PubMed]

Kanwisher, N., Chun, M. M., McDermott, J., & Ledden, P. J. (1996). Functional imagining of human visual recognition. *Cognitive Brain Research, 5*, 55–67. [PubMed]

Kleinschmidt, A., Buchel, C., Zeki, S., & Frackowiak, R. S. (1998). Human brain activity during spontaneously reversing perception of ambiguous figures. *Proceedings of the Royal Society B Biological Sciences, 265*, 2427–2433. [PubMed] [Article]

Konen, C. S., & Kastner, S. (2008). Two hierarchically organized neural systems for object information in human visual cortex. *Nature Neuroscience, 11*, 224–231. [PubMed]

Kourtzi, Z., Erb, M., Grodd, W., & Bulthoff, H. H. (2003). Representation of the perceived 3-D object shape in the human lateral occipital complex. *Cerebral Cortex, 13*, 911–920. [PubMed] [Article]

Kourtzi, Z., & Kanwisher, N. (2000). Cortical regions involved in perceiving object shape. *Journal of Neuroscience, 20*, 3310–3318. [PubMed] [Article]

Kourtzi, Z., Krekelberg, B., & van Wezel, R. J. (2008). Linking form and motion in the primate brain. *Trends in Cognitive Sciences, 12*, 230–236. [PubMed]

Freeman, Sterzer, & Driver

Kriegeskorte, N., Simmons, W. K., Bellgowan, P. S., & Baker, C. I. (2009). Circular analysis in systems neuroscience: the dangers of double dipping. *Nature Neuroscience, 12*, 535–540. [PubMed]

Kriegeskorte, N., Sorger, B., Naumer, M., Schwarzbach, J., van den Boogert, E., Hussy, W., et al., (2003). Human cortical object recognition from a visual motion flowfield. *Journal of Neuroscience, 23*, 1451–1463. [PubMed] [Article]

Leopold, D. A., & Logothetis, N. K. (1996). Activity changes in early visual cortex reflect monkeys' percepts during binocular rivalry. *Nature, 379*, 549–553. [PubMed]

Leopold, D. A., & Logothetis, N. K. (1999). Multistable phenomena: changing views in perception. *Trends in Cognitive Sciences, 3*, 254–264. [PubMed]

Likova, L. T., & Tyler, C. W. (2007). Stereomotion processing in the human occipital cortex. *Neuroimage, 38*(2), 293–305. [PubMed]

Lumer, E. D., Friston, K. J., & Rees, G. (1998). Neural correlates of perceptual rivalry in the human brain. *Science, 280*, 1930–1934. [PubMed]

Malach, R., Reppas, J. B., Benson, R. R., Kwong, K. K., Jiang, H., Kennedy, W. A., et al., (1995). Object-related activity revealed by functional magnetic resonance imaging in human occipital cortex. *Proceedings of the National Academy of Sciences USA, 92*, 8135–8139. [PubMed] [Article]

Mishkin, M., Ungerleider, L. G., & Macko, K. A. (1983). Object vision and spatial vision: two cortical pathways. *Trends in Neurosciences, 6*, 414–417.

Moore, C., & Engel, S. A. (2001). Neural response to perception of volume in the lateral occipital complex. *Neuron, 29*, 277–286. [PubMed]

Morrone, M. C., Tosetti, M., Montanaro, D., Fiorentini, A., Cioni, G., & Burr, D. C. (2000). A cortical area that responds specifically to optic flow, revealed by fMRI. *Nature Neuroscience, 3*, 1322–1328. [PubMed]

Moutoussis, K., Keliris, G., Kourtzi, Z., & Logothetis, N. (2005). A binocular rivalry study of motion perception in the human brain. *Vision Research, 45*, 2231–2243. [PubMed]

Muckli, L., Kriegeskorte, N., Lanfermann, H., Zanella, F. E., Singer, W., & Goebel, R. (2002). Apparent motion: event-related functional magnetic resonance imaging of perceptual switches and States. *Journal of Neuroscience, 22*, RC219. [PubMed] [Article]

Murray, S. O., Kersten, D., Olshausen, B. A., Schrater, P., & Woods, D. L. (2002). Shape perception reduces activity in human primary visual cortex. *Proceedings of the National Academy of Sciences USA, 99*, 15 164–15 169. [PubMed] [Article]

Murray, S. O., Olshausen, B. A., & Woods, D. L. (2003). Processing Shape, Motion and Three-dimensional Shape-from-motion in the Human Cortex. *Cerebral Cortex, 13*, 508–516. [PubMed] [Article]

Nawrot, M., & Blake, R. (1989). Neural integration of information specifying structure from stereopsis and motion. *Science, 244*, 716–718. [PubMed]

Niemeier, M., Goltz, H. C., Kuchinad, A., Tweed, D. B., & Vilis, T. (2005). A Contralateral Preference in the Lateral Occipital Area: Sensory and Attentional Mechanisms. *Cerebral Cortex, 15*, 325–331. [PubMed] [Article]

Ollinger, J. M., Shulman, G. L., & Corbetta, M. (2001). Separating processes within a trial in event-related functional MRI. *Neuroimage, 13*, 210–217. [PubMed]

Orban, G. A., Sunaert, S., Todd, J. T., Van, H. P., & Marchal, G. (1999). Human cortical regions involved in extracting depth from motion. *Neuron, 24*, 929–940. [PubMed]

Paradis, A. L., Cornilleau-Peres, V., Droulez, J., Van De Moortele, P. F., Lobel, E., Berthoz, A., et al., (2000). Visual perception of motion and 3-D structure from motion: an fMRI study. *Cerebral Cortex, 10*, 772–783. [PubMed] [Article]

Parker, A. J., & Newsome, W. T. (1998). Sense and the single neuron: probing the physiology of perception. *Annual Review of Neuroscience, 21*, 227–277. [PubMed]

Polonsky, A., Blake, R., Braun, J., & Heeger, D. J. (2000). Neuronal activity in human primary visual cortex correlates with perception during binocular rivalry. *Nature Neuroscience, 3*, 1153–1159. [PubMed]

Preston, T. J., Kourtzi, Z., & Welchman, A. E. (2009). Adaptive estimation of three-dimensional structure in the human brain. *Journal of Neuroscience, 29*, 1688–1698. [PubMed] [Article]

Qian, N., Andersen, R. A., & Adelson, E. H. (1994). Transparent motion perception as detection of unbalanced motion signals. I. Psychophysics. *Journal of Neuroscience, 14*, 7357–7366. [PubMed] [Article]

Raichle, M. E., MacLeod, A. M., Snyder, A. Z., Powers, W. J., Gusnard, D. A., & Shulman, G. L. (2001). A default mode of brain function. *Proceedings of the National Academy of Sciences USA, 98*, 676–682. [PubMed] [Article]

Rees, G., Friston, K., & Koch, C. (2000). A direct

quantitative relationship between the functional properties of human and macaque V5. *Nature Neuroscience, 3*, 716–723. [PubMed]

Small, D. M., Gitelman, D. R., Gregory, M. D., Nobre, A. C., Parrish, T. B., & Mesulam, M. M. (2003). The posterior cingulate and medial prefrontal cortex mediate the anticipatory allocation of spatial attention. *Neuroimage, 18*, 633–641. [PubMed]

Smith, A. T., Wall, M. B., Williams, A. L., & Singh, K. D. (2006). Sensitivity to optic flow in human cortical areas MT and MST. *European Journal of Neuroscience, 23*, 561–569. [PubMed]

Sterzer, P., Eger, E., & Kleinschmidt, A. (2003). Responses of extrastriate cortex to switching perception of ambiguous visual motion stimuli. *Neuroreport, 14*, 2337–2341. [PubMed]

Sterzer, P., Haynes, J. D., & Rees, G. (2006). Primary visual cortex activation on the path of apparent motion is mediated by feedback from hMT+/V5. *Neuroimage, 32*, 1308–1316. [PubMed]

Sterzer, P., & Kleinschmidt, A. (2005). A neural signature of colour and luminance correspondence in bistable apparent motion. *European Journal of Neuroscience, 21*, 3097–3106. [PubMed]

Sterzer, P., & Kleinschmidt, A. (2007). A neural basis for inference in perceptual ambiguity. *Proceedings of the National Academy of Sciences USA, 104*, 323–328. [PubMed] [Article]

Sterzer, P., Kleinschmidt, A., & Rees, G. (2009). The neural bases of multistable perception. *Trends in Cognitive Sciences, 13*, 310–318. [PubMed]

Sterzer, P., Russ, M. O., Preibisch, C., & Kleinschmidt, A. (2002). Neural correlates of spontaneous direction reversals in ambiguous apparent visual motion. *Neuroimage, 15*, 908–916. [PubMed]

Teo, P. C., Sapiro, G., & Wandell, B. A. (1997). Creating connected representations of cortical gray matter for functional MRI visualization. *IEEE Transactions on Medical Imaging, 16*, 852–863. [PubMed]

Tong, F., Nakayama, K., Vaughan, J. T., & Kanwisher, N. (1998). Binocular rivalry and visual awareness in human extrastriate cortex. *Neuron, 21*, 753–759. [PubMed]

Tootell, R. B., Reppas, J. B., Kwong, K. K., Malach, R., Born, R. T., Brady, T. J., et al., (1995). Functional analysis of human MT and related visual cortical areas using magnetic resonance imaging. *Journal of Neuroscience, 15*, 3215–3230. [PubMed] [Article]

Treue, S., Husain, M., & Andersen, R. A. (1991). Human perception of structure from motion. *Vision Research, 31*, 59–75. [PubMed]

Vanduffel, W., Fize, D., Peuskens, H., Denys, K., Sunaert, S., Todd, J. T., et al., (2002). Extracting 3D from motion: differences in human and monkey intraparietal cortex. *Science, 298*, 413–415. [PubMed]

Vogt, B. A., Finch, D. M., & Olson, C. R. (1992). Functional heterogeneity in cingulate cortex: the anterior executive and posterior evaluative regions. *Cerebral Cortex, 2*, 435–443. [PubMed] [Article]

Wallach, H., & O'Connell, D. N. (1953). The kinetic depth effect. *Journal of Experimental Psychology, 45*, 205–217. [PubMed]

Wandell, B. A., Chial, S., & Backus, B. T. (2000). Visualization and measurement of the cortical surface. *Journal of Cognitive Neuroscience, 12*, 739–752. [PubMed]

Watson, J. D., Myers, R., Frackowiak, R. S., Hajnal, J. V., Woods, R. P., Mazziotta, J. C., et al., (1993). Area V5 of the human brain: evidence from a combined study using positron emission tomography and magnetic resonance imaging. *Cerebral Cortex, 3*, 79–94. [PubMed] [Article]

Weigelt, S., Kourtzi, Z., Kohler, A., Singer, W., & Muckli, L. (2007). The cortical representation of objects rotating in depth. *Journal of Neuroscience, 27*, 3864–3874. [PubMed] [Article]

Welchman, A. E., Deubelius, A., Conrad, V., Bulthoff, H. H., & Kourtzi, Z. (2005). 3D shape perception from combined depth cues in human visual cortex. *Nature Neuroscience, 8*, 820–827. [PubMed]

Appendix

Movie demonstrations

Movies illustrating the two kinds of random-dot kinematograms used for cylindrical and flat stimuli: "cylinder.mov" and "flat.mov" respectively.